Journal of Neonatal Surgery
ISSN(Online): 2226-0439
Vol. 14,issue.32s (2025)
https://www.jneonatalsurg.com

OPEN ACCESS

Leaf extract from Costus pictus D.: Unveiling the power of synthesized TiO2 nanoparticles through phytochemical analysis and exciting Antiplatelet and Anticoagulant activity evaluations

Shalini KR[1], Udayakumar R[2*], Udhayan S[3]

[1,2*]Department of Physics, Annamalai University, Annamalai Nagar, Tamil Nadu, India

[3]Adhi College of Engineering and Technology, Department of Physics, Sankarapuram, Kanchipuram-631605, Tamil Nadu, India

***Corresponding author:**

Udayakumar R

Email ID: drru.krs24@gmail.com

Cite this paper as Shalini KR, Udayakumar R, and Udhayan S (2025) Leaf extract from Costus pictus D.: Unveiling the power of synthesized TiO2 nanoparticles through phytochemical analysis and exciting Antiplatelet and Anticoagulant activity evaluations. .Journal of Neonatal Surgery, 14, (32s), 9852-9872

ABSTRACT

The environmentally friendly synthesis of titanium dioxide (TiO_2) nanoparticles (NPs) utilizing the leaf extract of *Costus pictus* D. was accomplished to create sustainable and biologically active materials. This research involves the synthesis, characterization, and assessment of these nanoparticles' anticoagulant and antiplatelet properties. Various characterization methods, such as X-ray diffraction (XRD), Scanning electron microscopy (SEM), Fourier-transform infrared spectroscopy (FTIR), and Gas chromatography-masscrystalline nanoparticles enriched with bioactive compounds sourced from the plant extract. The synthesized TiO_2 nanoparticles demonstrated significant anticoagulant properties by by markedly prolonging clotting times and inhibiting intrinsic coagulation pathways. Additionally, these nanoparticles exhibited strong dose-dependent antiplatelet activity, showing superior efficacy compared to aspirin in inhibiting ADP-induced platelet aggregation. These findings underscore the potential therapeutic applications of *Costus pictus*- mediated TiO_2 nanoparticles in advancing cardiovascular health management. The study also emphasizes the importance of green synthesis as a sustainable and environmentally responsible methodology for developing nanoparticles in biomedical applications, highlighting the responsibility of researchers in the field.

1. INTRODUCTION

Nanotechnology, which entails the manipulation of materials at the nanoscale (1-100 nm), is revolutionizing numerous fields, such as medicine and environmental science. The Indian subcontinent has recently experienced significant growth in the natural product sector, fueled by an increasing preference for Ayurvedic and herbal remedies. This shift towards natural alternatives is driven by concerns over synthetic drugs side effects and environmental impact, reflecting a broader global trend towards health-conscious and eco-friendly choices [1]. The World Health Organization (WHO) acknowledges this development, observing the increasing incorporation of traditional medicine into global healthcare systems [2].

In this context, the green synthesis of nanoparticles has gained prominence for its environmentally friendly approach. This method utilizes natural substances, such as plant extracts, to produce nanoparticles, reducing the reliance on toxic chemicals and minimizing environmental impact [3]. Titanium dioxide (TiO_2) nanoparticles are notable among different types of nanoparticles because of their diverse applications and distinct characteristics. The anatase and rutile forms of TiO_2 nanoparticles are highly regarded for their photocatalytic effectiveness, durability, and non-toxic nature, which renders them appropriate for various uses in environmental and biomedical sectors [4].

The selection of *Costus pictus D.*, known as the insulin plant, for synthesizing TiO_2 nanoparticles is based on its traditional medicinal use and documented hypoglycemic effects. This plant, part of the Costaceae family, has been shown to enhance pancreatic insulin secretion

and beta-cell activity [5-7]. The choice leverages the plant's bioactive compounds to improve the synthesis and performance of the nanoparticles.

Recent WHO data underscores the critical role of anticoagulants and antiplatelet therapies in managing cardiovascular diseases, which are a leading cause of global morbidity and mortality. Cardiovascular diseases account for approximately 32% of all global deaths, translating to around 17.9 million deaths annually [8]. Among these conditions, thromboembolic events such as stroke and myocardial infarction are prevalent and contribute significantly to the global disease burden..

Specifically, stroke impacts around 15 million individuals globally each year, leading to an estimated 5 million fatalities and leaving an additional 5 million people with lasting disabilities [9]. Given this substantial impact, anticoagulants and antiplatelet agents are essential in preventing such events and improving patient outcomes. The WHO highlights the urgent need for effective and safe therapeutic options to address the substantial burden of cardiovascular diseases and enhance patient care [10-12].

Considering these worldwide health issues, this research intends to assess the anticoagulant and antiplatelet effects of TiO_2 nanoparticles synthesized using the leaf extract of *Costus pictus D*. This choice is justified by the growing demand for natural and less toxic alternatives for managing cardiovascular health. By investigating these properties, the study contributes to developing new, eco-friendly therapeutic options that align with global health priorities and sustainability goals.

The approach of green synthesis utilizing leaf extract from *Costus pictus* D. as a natural reducing and stabilizing agent reduces the reliance on harmful chemicals, thereby improving the environmental and economic sustainability of the nanoparticle production process. The research will include the synthesis of TiO_2 nanoparticles, their characterization via thermal, structural, and morphological assessments, and the execution of qualitative phytochemical analysis to determine the chemical components of the leaf extract. Furthermore, the anticoagulant and antiplatelet activities of the nanoparticles will be assessed to uncover their potential therapeutic applications

Experimental

2. MATERIALS:

Analytical grade titanium tetrafluoride (TiF_4) was employed to synthesize titanium dioxide (TiO_2) nanoparticles. For the Fourier Transform Infrared (FTIR) analysis, dry spectral grade potassium bromide (KBr) with a purity of 98.7% was utilized to prepare the pellets. Analytical reagent (AR) grade chemicals, including sodium hydroxide, sulfuric acid, glacial acetic acid, ferric chloride, hydrochloric acid, iodine solution, and chloroform, were procured from M/s Merck (Mumbai, India) to conduct qualitative phytochemical analysis of the test samples. Dichloromethane (DCM) and dimethyl sulfoxide (DMSO) solvents were sourced from M/s Sigma Aldrich (Mumbai, India). They were used for gas chromatography-mass spectrometry (GC-MS) and nuclear magnetic resonance (NMR) analyses. All glassware was thoroughly cleaned and dried in a hot air oven before use.

Collection of Plant Material:

The plant material, *Costus pictus* D., was collected from the Karaikudi region of Tamil Nadu, India. The leaves were then separated from the plant and thoroughly washed with running water. After this initial cleaning, the leaves were rinsed with distilled water, not just once or twice, but three to four times, ensuring the removal of any contaminants and leaving the plant material in a pristine state.

Preparation of Leaf Extract:

The leaf extract was obtained using a straightforward extraction technique. Fresh leaves of *Costus pictus* D. were cleaned thoroughly with distilled water, dried in a hot air oven, and powdered finely. Five grams of the precisely powdered leaves were mixed with 100 milliliters of distilled water in a beaker. The blend was heated to 80 °C for one hour. After heating, the crude extract was filtered through Whatman No. 1 filter paper and stored in the refrigerator for later use.

Synthesis of Titanium Dioxide (TiO_2) Nanoparticles:

Titanium dioxide (TiO_2) nanoparticles were produced by mixing 20 milliliters of leaf extract with 3.4 grams of titanium tetrafluoride (TiF_4) to create a 0.1 M solution. The mixture was then heated until the precipitates were dried at 100 °C for six hours. After drying, the precipitates were calcined at a temperature of 500 °C for one hour to yield TiO_2 nanoparticles [13]. (Fig. 1) illustrates the reaction mechanism for forming TiO_2 NPs using leaves from *Costus pictus D.*

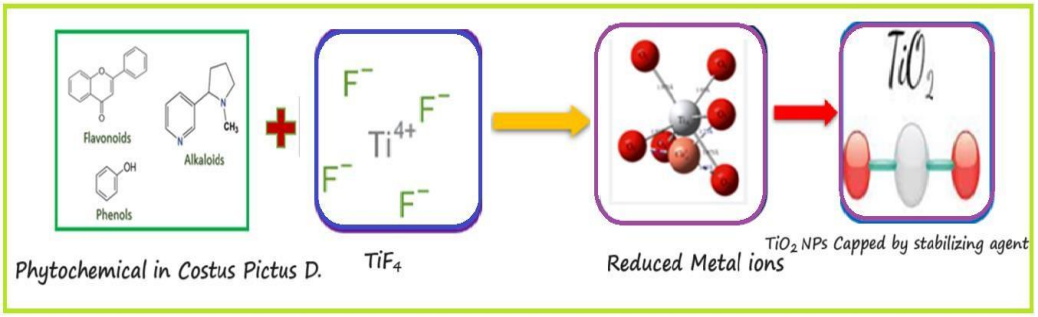

Fig. 1. Reaction mechanism for synthesizing CP @ TiO2 nanoparticles (NPs).

Instrumentation:

Thermal Analysis: The thermal characteristics of the nanoparticles were carefully analyzed using a NETZSCH-STA 449 F3 JUPITER device in an inert atmosphere at a controlled heating rate of 20 °C/min, which guaranteed the precision of the findings in the current study.

Structural Analysis: The structural characterization was performed using a SHIMADZU XRD 6000 X-ray diffractometer that utilized Cu Kα radiation (1.5406 Å). The X-ray tube functioned at 40 kV and 30 mA, with a step scanning rate of 0.05 seconds, facilitating a thorough comprehension of the nanoparticles' structure.

Morphological Analysis: The size and shape of the nanoparticles were accurately assessed using Scanning Electron Microscopy (SEM) with the JOEL JSM-IT 200 device, which offered a clear visual depiction of the nanoparticles.

Functional Group Analysis: Fourier Transform Infrared Spectroscopy (FTIR) measurements were conducted using a Nicolet iS5 system. Around 2 mg of TiO_2 nanoparticles were mixed with KBr to create pellets, which were then scanned across the 4000 to 400 cm-1 range.

Phytochemical Analysis: Qualitative phytochemical analysis followed standard test procedures outlined in the literature [14].

GC-MS Analysis: Gas Chromatography-Mass Spectrometry (GC-MS) was performed using a Perkin Elmer GC model Clarus 680 and a Clarus 600 mass spectrometer.

NMR Analysis: Nuclear Magnetic Resonance (NMR) investigations were conducted using a BRUKER AVANCE I NMR spectrometer operating at 400 MHz.

Assessment of Anticoagulant Activity:

The anticoagulant effect was evaluated by measuring Activated Partial Thromboplastin Time (APTT) and Prothrombin Time (PT).

For the APTT test, 90 µL of citrated normal human plasma was combined with 10 µL of the sample, followed by a one-minute incubation period at 37 °C. Subsequently, 100 µL of the APTT assay reagent was added, and the resulting mixture was subjected to an additional one- minute incubation at 37 °C. After this incubation, 100 µL of 20 mM $CaCl_2$ was introduced, and the clotting time was measured.

In the PT assay, 90 µL of citrated normal human plasma was mixed with 10 µL of the sample and incubated for one minute at 37 °C. Following this initial incubation, 200 µL of the PT assay reagent, preincubated for ten minutes at 37 °C, was added, and the clotting time was recorded. Anticoagulant activity was assessed by analyzing the results from both the APTT and PT tests.

Assessment of Antiplatelet Activity:

The evaluation of platelet aggregation was conducted with precision, commencing with the centrifugation of blood samples at 1500 g for 10 minutes to achieve separation of platelet- poor plasma. The plasma samples were subsequently transferred into plain tubes for immediate utilization at room temperature within three hours or stored by freezing at -80 °C for up to six months. For the platelet aggregation assay, 100 µL of the plasma sample at concentrations of 5,10, 25, 50, and 100 µL was combined with 200 µL of a phosphate-buffered saline (PBS) diluent. This mixture was incubated at 37 °C for four minutes before adding adenosine diphosphate (ADP) at a concentration of 10 µM, which served as the agonist. Measurements of platelet aggregation were conducted at a wavelength of 550 nm. Diluted whole blood functioned as the control, while aspirin was the positive control. The percentage of inhibition was calculated utilizing the following formula:

Percentage inhibition = $(Abs_{test} / Abs_{control}) \times 100$.

3. RESULTS & DISCUSSION

Thermogravimetric Analysis and Differential Thermal Analysis (TG - DTA):

The thermal properties of the produced nanoparticles were assessed using Thermogravimetric Analysis (TGA) and Differential Thermal Analysis (DTA) within a temperature span of 30 ºC to 800 ºC, employing a heating rate of 20 ºC per minute in a nitrogen atmosphere. (Fig. 2) depicts the TGA-DTA curve obtained for the synthesized TiO_2 nanoparticles.

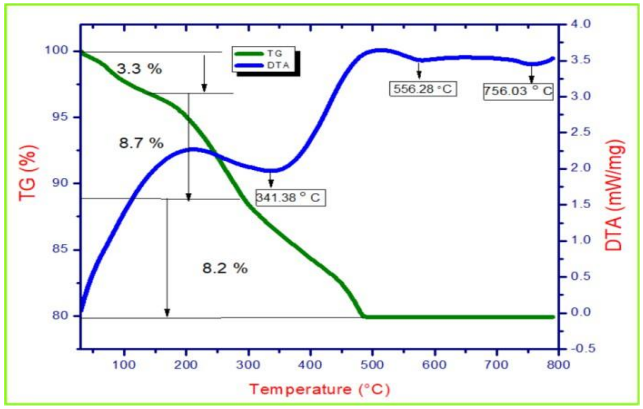

Fig. 2. TG-DTA curve for the as-prepared sample of CP @ TiO2 NPs (before calcination).

The TGA curve indicates the weight reduction of the biosynthesized sample, while the DTA curve shows the energy fluctuations throughout the thermal decomposition process. The breakdown of the TiO2 nano sample took place in three separate phases. The first phase, identified between room temperature and 140 °C, resulted in a weight decrease of around 3.3%, ascribed to the evaporation of loosely bound water molecules. This weight loss primarily stemmed from removing both physically and chemically attached water.

The second phase occurred from 140 °C to 304 °C, during which a weight reduction of about 8.7% was noted. This loss is linked to the pyrolysis and carbonization of biomass, as cited by Mishra et al. [15].

In the third phase, an additional weight decreases of roughly 8.2% was recorded between 304 °C and 480 °C. This temperature interval, which corresponds to a significant exothermic peak in the DTA curve, is related to the breakdown of chemically bound chromophoric groups and leftover organic components, including phytochemicals adsorbed on the nanoparticle surface. Ramimoghadam et al. observed comparable results, confirming the findings presented in this research [16].

Ray Diffraction (XRD) Analysis:

To investigate the crystallographic structure of the titanium dioxide (TiO2) nanoparticles synthesized using *Costus pictus* D. (CP) as a bioagent, an X-ray diffraction (XRD) spectrum was recorded within a 2θ range of 10 to 80 degrees. The XRD spectrum of CP @ TiO2 nanoparticles, calcined at 500 ºC, is presented in (Fig. 3)

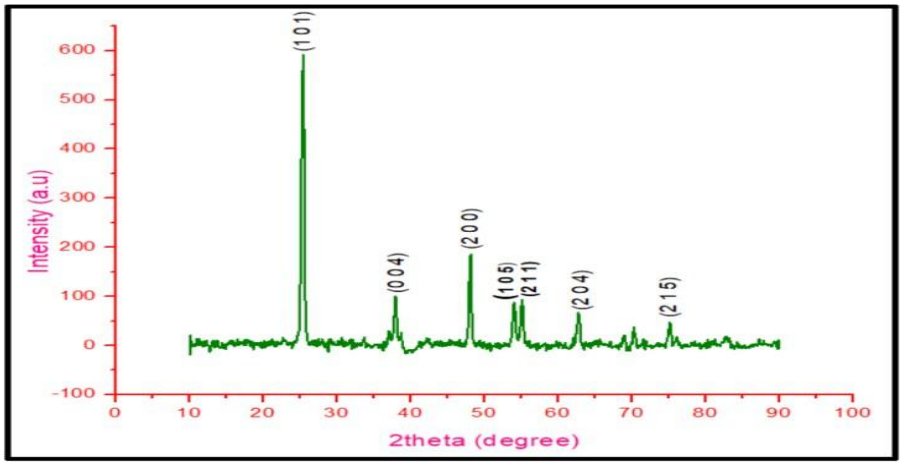

.Fig. 3. XRD Pattern recorded for CP @ TiO2 NPs.

The analysis revealed distinct diffraction peaks at approximately 2θ values of 25.1°, 37.6°, 48.3°, 53.9°, 55.4°, 63.04°, and 75.10°, which correspond to the Miller index planes (1 0

, (0 0 4), (2 0 0), (1 0 5), (2 1 1), (2 0 4), and (2 1 5), respectively. These findings confirm that the biosynthesized titanium dioxide nanoparticles exhibit a tetragonal crystal structure with no detectable impurities, in alignment with JCPDS card No.

21-1272.

Previous studies conducted by Bekele et al. and Ngoepe et al. have also examined the X-ray diffraction (XRD) characteristics of titanium dioxide (TiO_2) nanoparticles [17,13]. Their analyses reported significant diffraction peaks at various 2θ values, further confirming the presence of TiO_2 nanoparticles with a tetragonal crystalline structure consistent with the anatase phase of TiO_2, as supported by the JCPDS standard 21-1272.

Table - 1 presents the crystallite size (D), microstrain (ε), and dislocation density (δ) computed using Scherrer's formula. The average values obtained for D and ε were approximately 19 nm and 0.2703, respectively. Furthermore, Table - 2 offers a comparative analysis of the current XRD findings alongside those reported in earlier studies.

TABLE – 1 CRYSTALLOGRAPHIC STRUCTURAL CHARACTERISTICS COMPUTED FOR *COSTUS PICTUS* D.- INDUCED TiO_2 NANOPARTICLES

Position (2θ)	(h k l)	FWHM (β) (μm)	d-spacing (Å)	Crystallite size (D) [$\times 10^{-9}$m]	Microstrain (Ɛ) [$\times 10^{-3}$]	Dislocation density (δ) [$\times 10^{14}$]
25.12 º	(1 0 1)	0.43903	3.5422	18.09	0.5006	3.055
37.60 º	(0 0 4)	0.43464	2.3902	18.27	0.3311	2.99
48.38 º	(2 0 0)	0.38978	1.8886	20.38	0.2307	2.407
53.95 º	(1 0 5)	0.47015	1.6981	17.08	0.2496	3.427
55.42 º	(2 1 1)	0.4335	1.66404	18.32	0.2240	2.979
63.04 º	(2 0 4)	0.45418	1.4776	17.49	0.2064	3.269
75.10 º	(2 1 5)	0.39889	1.26205	19.91	0.1521	2.522

Mean D = 19 $\pm$ 1.141 nm; Mean Ɛ = 0.2703 $\pm$ 0.299 $\times 10^{-3}$

TABLE – 2 COMPARATIVE ANALYSIS OF XRD RESULTS FOR CP @ TiO_2 NANOPARTICLES IN RELATION TO PREVIOUS STUDIES

S. No.	Detected Nano particle	Precursor	Bioagent	Structure	JCPDS No.	Crystallite size (nm)	Reference
1	TiO_2	TiO_2	*Coleus aromaticus*	Tetragonal	04-0783	-	[18]
2	TiO_2	TTIP	*Mulberry plant*	Tetragonal	78-2486	22	[19]
3	TiO_2	$TiCl_4$	*Aloe barbadensis*	Tetragonal	21-1272	20	[20]
4	TiO_2	Titanium oxy sulphate	*Trigonella foenum*	Tetragonal	21-1272	25	[21]

5	TiO2	TiO2	*Andrographis paniculata*	Tetragonal	21-1272	23	[22]
6	TiO2	TiF4	*Costus pictus* D.	Tetragonal	84-1286	19	Present work

(Fig. 4) illustrates the Williamson-Hall (W-H) plot applicable to the CP @ TiO_2 nanocrystals. The values for crystallite size (D) and microstrain (ε) determined through the W-H method demonstrated strong concordance with those obtained from Scherrer's formula, as indicated in Table - 3. The absence of diffraction peaks corresponding to additional phases within the recorded X-ray spectrum further corroborates that the synthesized material exists in a pure phase of titanium dioxide nanoparticles characterized by a tetragonal structure.

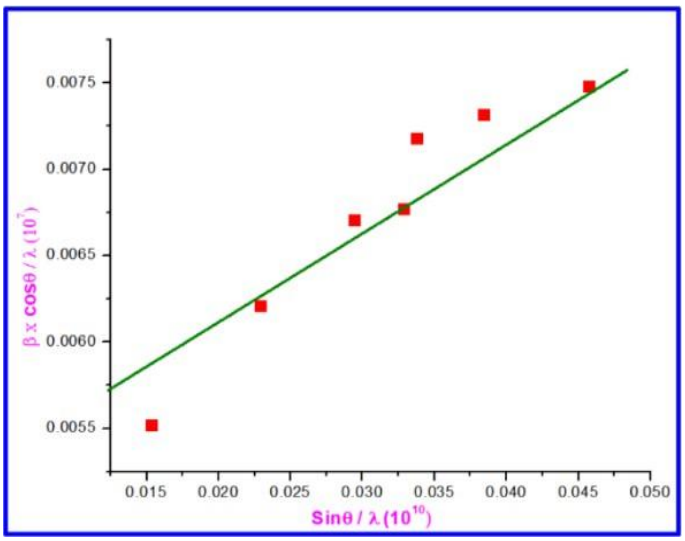

Fig. 4. W-H plot for CP @TiO2 NPs.

TABLE – 3 COMPARISON OF CRYSTALLINE STRUCTURAL DATA CALCULATED FOR CP @ TiO2 NANOPARTICLES

S. No.	Method	Crystallite size (nm)	Microstrain (Ɛ) [$\times 10^{-3}$]
1	Debye Scherrer	19	0.2703
2	W-H	22	0.2041

Morphological Analysis:

The shape, morphology, and apparent grain size of the synthesized TiO_2 nanoparticles were examined using Scanning Electron Microscopy (SEM). (Fig. 5a and 5b) display the nanoparticles' low - and high-magnification SEM images.

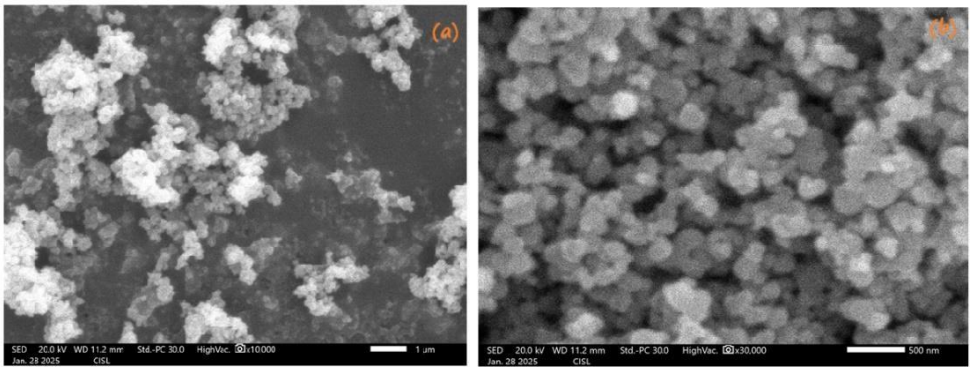

Fig. 5. SEM: Micrograph of the prepared CP @ TiO2 NPs

(Fig. 5b) shows that the nanoparticles are evenly distributed and possess a spherical shape, measuring 23 nm in size. Similar observations regarding the spherical morphology of TiO_2 nanoparticles were documented by Ansari et al. [23]. They investigated the morphology of biosynthesized TiO_2 nanoparticles from A. calamus plant leaf extract. They found the synthesized nanoparticles to be uniformly dispersed, spherical, and interconnected, with an average size ranging from 11 to 30 nm.

The elemental makeup of the synthesized nanoparticles was assessed using Energy- Dispersive X-ray Spectroscopy (EDS). The EDS spectrum illustrated in (Fig. 6) verifies the detection of titanium and oxygen as the only elements present, with no signs of impurities.

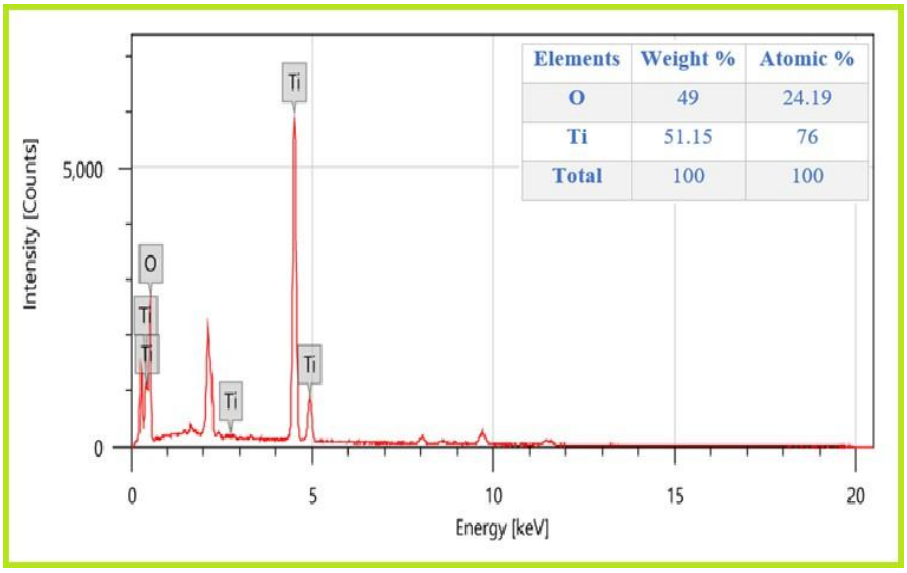

Fig. 6. EDS: Spectrum for the prepared CP @ TiO2 NPs.

The inset of (Fig. 6) presents the weight and atomic percentages of Ti and O, which further confirm the creation of pure anatase TiO_2. A similar finding was reported by Nabi et al. which highlighted the presence of Ti and O [24]. EDS analysis indicated that the peaks associated with titanium were notably intense, while the oxygen peaks exhibited relatively lower intensity. Furthermore, EDS analysis indicated the creation of non-stoichiometric TiO_2 nanoparticles with oxygen vacancies. These oxygen vacancies are anticipated to enhance the performance of the nanoparticles for the intended application, particularly in antibacterial activity within this study.

FTIR Spectral Analysis:

An aqueous leaf extract was subjected to analysis using Fourier Transform Infrared (FTIR) spectroscopy to investigate the bioactive compounds present in the leaves of *Costus pictus* D. This analysis was similarly conducted on both the as-synthesized (prior to calcination) and biosynthesized (post-calcination) TiO_2 nano samples. The FTIR spectra were recorded in the 4000 cm^{-1} to 400 cm^{-1} range. (Fig. 7a) presents the FTIR spectrum for the crude leaf extract, while Table - 4(a) delineates the tentative assignments of various functional groups identified within the spectrum. A thorough examination

of Table - 4(a) reveals the presence of functional groups associated with various phytochemical compounds, including phenols, tannins, and anthraquinones, as noted by Bekele et al. [17].

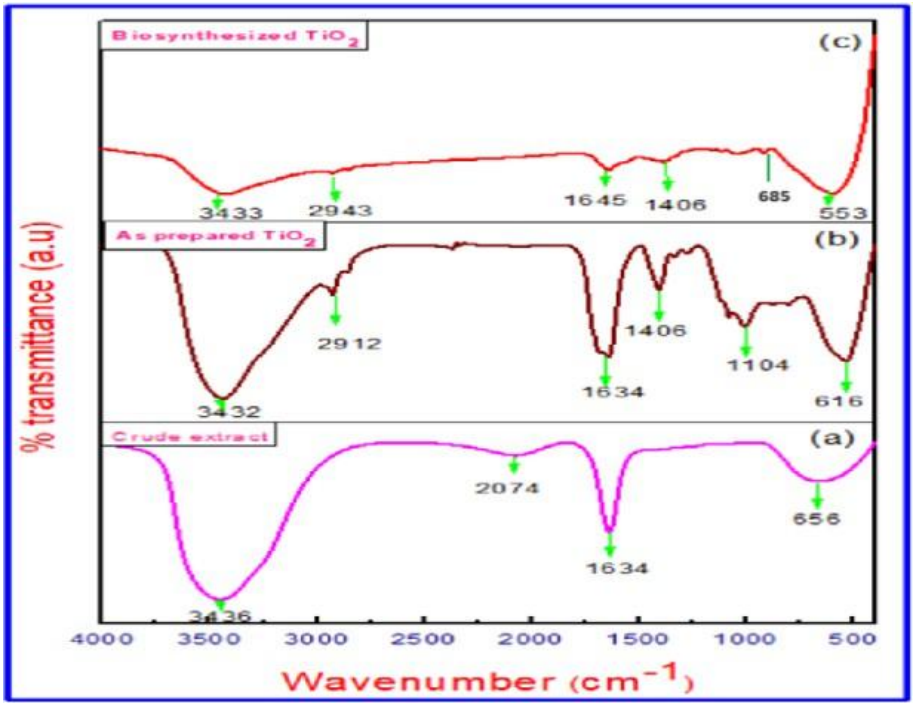

Fig.7. FTIR spectra for (a) crude extract of *Costus pictus D.* leaves, (b) as-prepared TiO2 nanoparticles, and (c) CP D.-mediated TiO2 NPs.

TABLE – 4 TENTATIVE ASSIGNMENTS FOR THE PEAKS OBSERVED IN THE FTIR SPECTRA

(a) Crude leaf extract of *Costus pictus* D. Leaves		
S. No.	Peak value (cm^{-1})	Tentative Assignment
1	3436	O-H stretching (Phenols)
2	2074	C-H stretching (Tannins)
3	1634	C=O (Anthraquinones)
4	656	M-O stretching frequency
(b) Pre calcination sample		
S. No.	Peak value (cm^{-1})	Tentative Assignment
1	3432	O-H stretching (Phenols)
2	2912	Alkyl chain (Alkaloids)

3	1634	C=O (Anthraquinones)
4	1406	C-H stretching (Tannins)
5	1104	C-O stretching vibration (Aromatic groups)
6	616	Ti-O-Ti bond
(c) Post calcination sample		
S. No.	Peak value (cm^{-1})	Tentative Assignment
1	3433	O-H stretching (Phenols)
2	2943	Alkyl chain (Alkaloids)
3	1645	C=O (Anthraquinones)
4	1406	C-H stretching (Tannins)
5	685	Ti-O-Ti bond
6	553	Formation of O-Ti-O

(Fig. 7b) illustrates the FTIR spectrum for the as-synthesized sample, synthesized utilizing *Costus pictus* D. leaf extract. Table - 4(b) offers the tentative assignments for the distinct FTIR peaks observed in this spectrum. It is apparent from Table - 4(b) that, in addition to the functional groups attributed to phytochemicals such as phenols, anthraquinones, and tannins, alkaloids, aromatic structures, and the Ti-O-Ti bond has also been detected. The FTIR spectrum for CP @ TiO_2 nanoparticles (i.e., post-calcination) was recorded, revealing the presence of several functional groups. These findings are detailed in (Fig. 7c) and Table - 4(c), which

provide a comprehensive overview of the identified functional groups in the spectrum. The FTIR spectrum for the CP @ TiO_2 nanoparticles exhibited a prominent peak at 3430 cm^{-1}, attributable to OH stretching associated with phenols. Absorption peaks at 2943 cm^{-1} and 1645 cm^{-1} are likely due to alkyl chains and the C=O bond related to anthraquinones, respectively. The peak at 1406 cm^{-1} may also correspond to C-H bending in tannins. The significant band at 553 cm^{-1} corroborates the presence of TiO_2 nanoparticles, as noted by George et al. [25]. Table - 5 presents a comparative analysis of the FTIR results alongside findings from previously reported studies.

TABLE – 5 COMPARATIVE EXAMINATION OF FTIR ANALYSIS RESULTS WITH FINDINGS FROM PRIOR RESEARCH

S. No.	Bioagent	Identified Phytochemicals	Reference
1	*Juniperus phoenicea* leaf	Phenols, Aromatic compounds and Vitamins	Masoudi et al. [26]
2	*Mulberry* plant extract	Phenols, Anthraquinones, Alkaloids and Tannins	Shimi et al. [27]

3	*Trigonella foenum- graecum*	Phenols, Alkaloids, Anthraquinones and Vitamins	Subhapriya et al. [21]
4	*Costus pictus* D.	Phenols, Anthraquinones and Tannins	Present work

TABLE – 6 SUMMARY OF THE CURRENT FTIR ANALYSIS OUTCOMES

Phytochemical present		Available in	
	Crude Sample	Before calcination sample	After calcination sample
Phenols	+	+	+
Alkaloids	-	+	+
Anthraquinones	+	+	+
Aromatic compounds	-	+	-
Tannins	+	+	+

(+) indicates presence; (-) indicates absence;

As indicated in Table - 6, phenols, anthraquinones, and tannins are consistently present across all three samples: the aqueous leaf extract, the as-synthesized nanomaterial, and the CP @ TiO_2 nano sample.

Qualitative Phytochemical Analysis:

The qualitative phytochemical screening of the aqueous leaf extract, as-synthesized TiO_2 nanosample (prior to calcination), and biosynthesized TiO_2 nanosample (after calcination) was conducted utilizing established methodologies. The results of this investigation are summarized in Table - 7. A thorough analysis of Table - 7 indicates that the crude leaf extract is comprised of several phytochemicals, including alkaloids, anthocyanins, betacyanin, cardiac glycosides, carbohydrates, coumarins, steroids, glycosides, phenols, and tannins. The as-synthesized TiO_2 nanosample exhibited the presence of alkaloids, phenols, and tannins, while the biosynthesized TiO_2 nanosample retained many of these compounds. These findings validate and significantly contribute to the results reported by Ahmad et al. [19], who similarly identified the presence of these phytochemicals in TiO_2 nanoparticles synthesized from various plant extracts.

TABLE – 7 QUALITATIVE PHYTOCHEMICAL ANALYSIS OF CRUDE LEAF EXTRACT, AS-SYNTHESIZED SAMPLE, AND BIOSYNTHESIZED TiO_2 NANOPARTICLES

S. No.	Identified Phytochemicals		Test Sample	

		Leaf extract	Before calcination	After calcination
1	Alkaloids	+	+	+
2	Anthocyanins and Betacyanin	+	-	-
3	Cardiac glycosides	+	+	+
4	Carbohydrates	+	+	+
5	Coumarins	+	-	-
6	Flavonoids	-	+	-
7	Glycosides	+	+	+
8	Phenols	+	+	+
9	Steroids	+	-	-
10	Tannins	+	+	+
11	Terpenoids	-	-	-

(+) indicates presence; (-) indicates absence;

Gas Chromatography-Mass Spectrometric (GC-MS) Analysis:

The pivotal GC-MS analysis, a cornerstone of the present research, was instrumental in identifying the bioactive compounds in the crude leaf extract and titanium dioxide (TiO_2) nano- samples before and after calcination. This qualitative study involved comparing the retention times and mass spectra obtained for the selected samples with the collective database established by the National Institute of Standards and Technology (NIST).

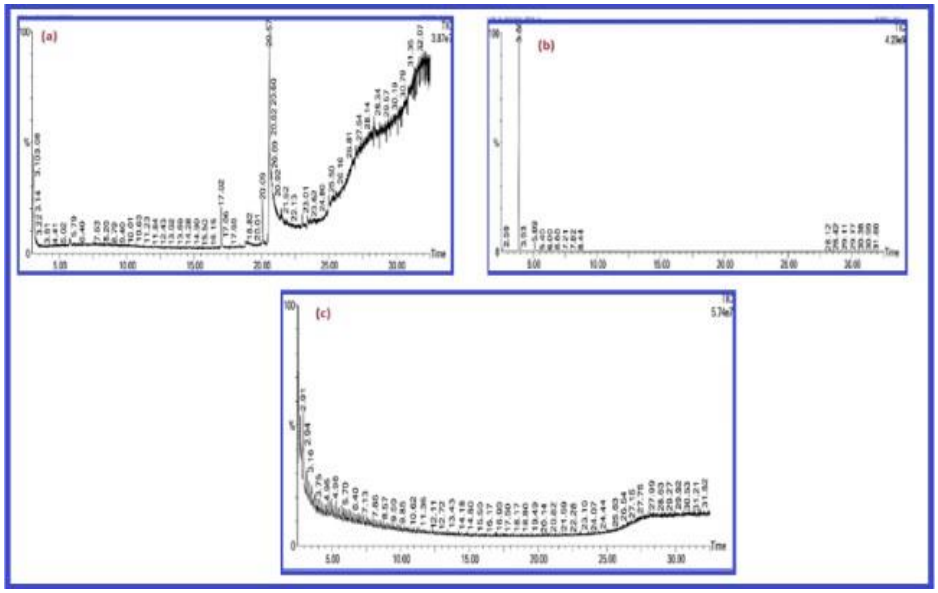

Fig. 8. (a) GC-MS chromatogram for the crude extract of *Costus pictus* (b) as- synthesized TiO_2 nanosample, and (c) biosynthesized TiO_2 NPs.

TABLE – 8 GC-MS ANALYSIS OF CRUDE LEAF EXTRACT FROM *COSTUS PICTUS* D. CHARACTERIZATION OF THE AS-PREPARED NANOPARTICLE SAMPLE ANALYSIS OF BIOSYNTHESIZED TiO_2 NANOPARTICLES

(a) Crude Leaf extract				
S. No.	RT (min.)	Identified Component	Formula	Bioactivity
1	3.083	Propenamide,2-Hydroxy	$C_3H_8O_2$ (Phenols)	Antihistaminic and Anticholinergic
2	3.158	Methane, Chloromethoxy	C_2H_5OCl (Glycosides)	Antibacterial and Anti -inflammatory activity
3	17.019	D-Proline	$C_5H_9O_2N$ (Steroids)	Antibacterial and Antifungal
4	20.085	Methylene Asparagine	$C_5H_8O_3N_2$ (Steroids)	Anticancer activities
5	20.571	But-2-Enoic Acid	$C_9H_{15}O_3N_3$ (Tannins)	Anti-inflammatory, and Antimicrobial activity.
6	31.415	Trans-2,3-Epoxynonane	$C_9H_{18}O$ (Coumarins)	Anticancer activity
7	31.650	Dl-Citrulline	$C_6H_{13}O_3N_3$ (Betacyanin)	Anti-inflammatory and Anticancer activity
8	31.715	3-Azonia-5-Hexene-1-Ol, N, N'-Dimethyl, Carbamate Ester, Bromide	$C_8H_{17}O_2N_2$ (Amino acids)	Antimicrobial activity
9	32.410	4-Hydroxylysine	$C_6H_{14}O_3N_2$ (Alkaloids)	Antioxidant and Anticancer activity
(b) As-synthesized nano sample				
S. No.	RT (min.)	Identified Component	Formula	Bioactivity
1.	3.879	Propanedioic Acid, Oxo-, Dimethyl Ester	$C_5H_6O_5$ (Tannins)	anti-hypertensive

2.	5.094	Propanedioic Acid, Oxo-, Ethyl Methyl Ester	$C_6H_8O_5$ (Alkaloids)	Antibacterial activity
(c) Biosynthesized TiO_2 NPs				
S. No.	RT (min.)	Identified Component	Formula	Bioactivity
1	2.563	Acetic Acid, Dichloro-, Methyl Ester	$C_3H_4O_2Cl_2$ (Coumarins)	Antibacterial and Antioxidant activity
3	2.914	1,6;3,4-Dianhydro-2- Deoxy, Beta-Dribo-Hexopyranosse	$C_6H_8O_3$ (Alkaloids)	Antibacterial activity
4	3.149	Methane, Bromodichloro	$CHCl_2Br$ (Carbohydrates)	Anthelminthic
5	3.359	Methane, Oxybis [Dichloro-	$C_2H_2OCl_4$ (Glycosides)	wound healing

(Fig. 8) illustrates the chromatograms corresponding to the crude leaf extract, as- synthesized TiO_2 nanoparticles, and biosynthesized TiO_2 nanoparticles. Table - 8 enumerates the compounds identified in each of these samples.

The crude leaf extract's GC-MS analysis revealed the presence of various bioactive compounds, including alkaloids, phenols, glycosides, tannins, coumarins, and amino acids. Several phytochemicals were also detected in the as-synthesized and biosynthesized TiO_2 nano samples, indicating their potential involvement in the synthesis process. This finding underscores the significant role of the GC-MS analysis in understanding the bioactivity and stability of the nanoparticles, consistent with observations from previous research studies [28-30].

TABLE – 9 Summary of the current GC-MS analysis outcomes

Phytochemical constituents		Available in	
	Crude leaf extract	As-synthesized nanosample	Biosynthesized TiO_2 nanosample
Phenols	+	-	-
Glycosides	+	-	+
Steroids	+	-	-
Tannins	+	+	+
Alkaloids	+	+	+

(+) indicates presence; (-) indicates absence;

From Table - 9, it is apparent that tannins and alkaloids are consistently present in all three selected samples: the aqueous leaf extract, as-synthesized TiO_2 nanoparticles (prior to calcination), and biosynthesized TiO_2 nanoparticles (after calcination). This significant observation emphasizes the critical role of these phytochemicals in the development of *Costus pictus*-mediated TiO_2 nanoparticles. Consequently, these nanoparticles, with their anticipated remarkable antimicrobial, antioxidant, anticancer, anti-inflammatory, antiplatelet, anticoagulant, and other biologically relevant activities,

underscore their substantial potential for various biomedical and therapeutic applications, sparking excitement about the possibilities of this research.

Nuclear Magnetic Resonance (NMR) Spectroscopy:

^{1}H NMR spectroscopy was conducted on the crude leaf extract, the as-synthesized nanomaterial, and the biosynthesized TiO2 nanoparticles to characterize the phytochemicals present. (Fig. 9) illustrates the NMR spectra, while Table - 10 summarizes the chemical shifts and assignments. The ^{1}H NMR spectra of both the crude leaf extract and the TiO2 nanomaterials (prior to and following calcination) exhibit peaks indicative of tannins, phenols, and alkaloids.

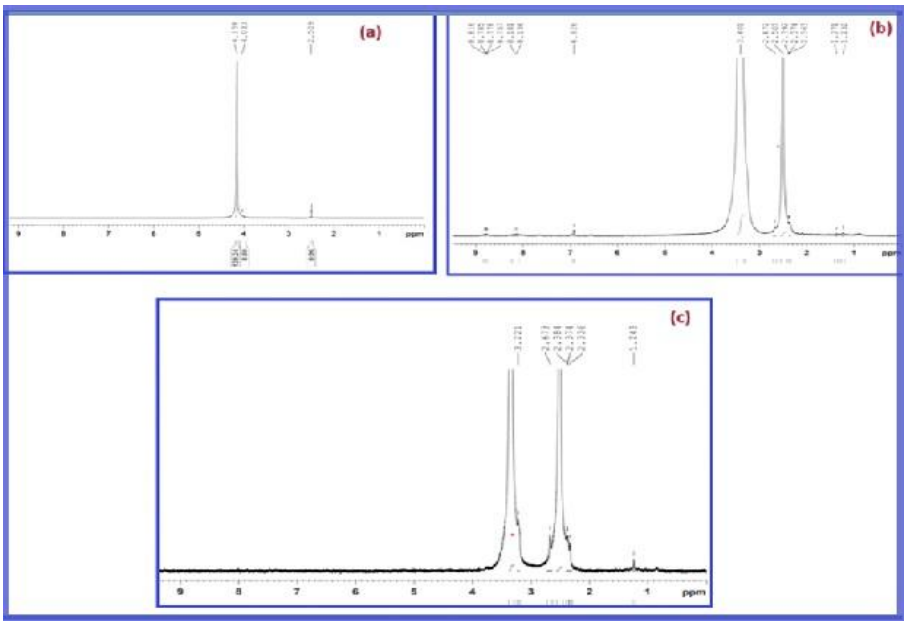

Fig. 9. ^{1}H NMR spectrum for (a) aqueous leaf extract of *Costuspictus D.*, (b) as-prepared TiO2 nanosample, and (c) biosynthesized TiO2 NPs.

TABLE – 10 TENTATIVE ASSIGNMENTS FOR THE ^{1}H NMR SPECTRUM OF (A) AQUEOUS LEAF EXTRACT OF *COSTUS PICTUS* D. (B) AS-PREPARED SAMPLE (BEFORE CALCINATION) (C) BIOSYNTHESIZED TiO2 NANOPARTICLES (AFTER CALCINATION)

(a) Crude leaf extract of *Costus pictus D.*			
S. No.	Peak identified (ppm)	Tentative Assignment	Probable Phytochemical Present
1.	2.509	Alcoholic Compound	Tannins
2.	4.033 and 4.158	Ar OH	Phenols
(b) Before calcination			
S. No.	Peak identified (ppm)	Tentative Assignment	Probable Phytochemical Present

1.	1.232 and 1.371	R- OH alcoholic Compound	Alkaloids
2.	2.363, 2.374, 2.392, 2.507, 2.672	Alcoholic compound	Tannins
3	3.401	N- CH3 moieties resonate	Flavonoids
4	8.136, 8.181, 8.75,8. 778, 8.785 and 8.816	Aromatic phenyl rings	Phenols
(c) After calcination			
S. No.	Peak identified (ppm)	Tentative Assignment	Probable Phytochemical Present
1	1.243	R - OH alcoholic	Alkaloids
		Compounds	
2	2.336, 2.374, 2.384 and 2.673		
		Alcoholic Compound	Tannins
3	3.221	N-CH3 moieties Resonates	Flavonoids

These findings are consistent with observations reported by previous researchers [31,32]. Identifying these phytochemicals in the nanoparticles indicates their potential contribution to the stabilization and bioactivity of the TiO_2 nanoparticles.

Table - 10 confirms the presence of tannins across all three selected samples: the crude leaf extract, the as-synthesized material (prior to calcination), and the biosynthesized product (post-calcination). This consistent observation underscores the essential and informative role that tannins play in the formation of TiO_2 nanoparticles induced by *Costus pictus* D. Furthermore, Table - 11 distinctly illustrates that tannins are present in all three analyzed samples, reinforcing their significant involvement in the synthesis of TiO_2 nanomaterials derived from *Costus pictus* D.

TABLE – 11 SUMMARY OF THE CURRENT ^{1}H NMR ANALYSIS OUTCOMES

Phytochemical constituents		Available in	
	Crude leaf extract	As-synthesized nanosample	Biosynthesized TiO_2 nanosample
Alkaloids	-	+	+
Flavonoids	-	+	+

Phenols	+	+	
Tannins	+	+	+

(+) indicates presence; (-) indicates absence;

Anticoagulant activity:

The coagulation system is essential for maintaining stable blood flow by preventing excessive bleeding while supporting the innate immune system in limiting the dissemination of infectious agents. Furthermore, infection-related blood clots can lead to tissue damage. They may result in organ failure, a condition frequently associated with cardiovascular diseases, autoimmune responses, allergic reactions, traumas, and the progression of cancer [33]. There is substantial evidence indicating that nanoparticles possess the potential to enhance the efficacy of conventional anticoagulant agents, thereby mitigating the risks associated with high drug concentrations and reducing the overall cost of treatment, including the frequency of administration.

While titanium dioxide (TiO_2) nanoparticles represent a promising alternative to traditional anticoagulants, potentially diminishing the risks and limitations of standard treatment modalities, it is important to note that there may be some associated risks. These could include potential toxicity, immune system response, or long-term effects that must be thoroughly investigated. The anticoagulant activity observed in these nanoparticle formulations is comparable to, and in some instances exceeds, the performance of widely used anticoagulants such as heparin.

The anticoagulant properties of TiO_2 nanoparticles synthesized from the leaves of the *Costus pictus* D. plant were systematically evaluated, with results summarized in Table - 12.

TABLE – 12 ASSESSMENT OF THE ANTICOAGULANT ACTIVITY OF CP @ TiO2 NANOPARTICLES

Sample (µg/ml)	PT/Clotting time (Second)
(a) Biosynthesized TiO_2	
10	25
25	44
50	68
100	83
(b) Heparin	116
100	

The synthesized nanoparticles demonstrated significant anticoagulant effects, particularly on the intrinsic pathway of the coagulation cascade. Notably, the CP @ TiO2 nanoparticles resulted in a moderate increase in prothrombin time (PT), indicating their effective interaction with components of the intrinsic pathway to inhibit clot formation. In vitro assays confirmed these anticoagulant properties, as shown in (Fig.10**)**, which details the blood coagulation effects of varying concentrations of *Costus pictus* D.-induced TiO_2 nanoparticles.

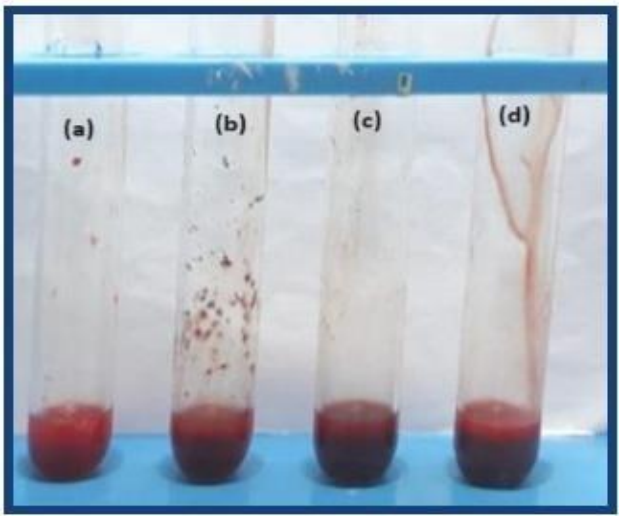

Fig. 10. Blood coagulation results for different concentrations of TiO2 NPs: (a) 10 µg/mL, (b) 25 µg/Ml, (c) 50 µg/mL, (d) 100 µg/mL.

The biosynthesized TiO2 nanoparticles, produced through the use of natural sources such as plant extracts or microorganisms to reduce and stabilize metal ions, were shown in in vitro studies to significantly elevate the prothrombin test (PT) clotting time from the control baseline of 25 seconds to 83 seconds, indicating a dose-dependent anticoagulant effect. While blood clotting is crucial for preventing hemorrhage, the timely and effective dissolution of clots is equally important for preventing thrombosis, maintaining hemostasis, and treating ischemia. These findings highlight the potential of TiO2 nanoparticles as an anticoagulant, though further investigation into their safety and efficacy is required before clinical application. Additionally, research by Kim et al. demonstrated that biosynthesized gold nanoparticles (AuNPs) using earthworm extract synergistically enhanced the anticoagulant properties of heparin by 118.9% [34]. Similarly, Elegbede et al. found that biosynthesized AuNPs utilizing xylanase facilitated

clot dissolution within five minutes when applied to preformed blood clots without exhibiting thrombolytic activity [35].

Antiplatelet Activity:

Platelets play a vital role in the bloodstream, particularly in blood clotting during injury. In physiological contexts, adenosine diphosphate (ADP) is an agonist that binds to specific receptors on the platelet membrane. This binding initiates a series of alterations that lead to platelet aggregation. Activated platelets are integral to forming clots at the injury site, establishing a structural mesh that effectively prevents blood loss during injury or disease [36].

The antiplatelet activity of *Costus pictus*-mediated titanium dioxide (TiO2) nanoparticles was evaluated, with comprehensive results in Table - 13 and illustrated in (Fig. 11). The nanoparticles exhibited a significant inhibition of ADP-induced platelet aggregation, achieving an inhibition rate of 98%. This performance notably surpassed standard aspirin treatment, demonstrating an inhibition rate of 96%. These results suggest that CP @ TiO2 nanoparticles could be a more effective antiplatelet agent than aspirin.

TABLE – 13 EVALUATION OF THE ANTIPLATELET ACTIVITY OF *COSTUS PICTUS* D.- INDUCED NANOPARTICLES

Concentration (µg/mL)	% of Platelet aggregation	% of inhibition
(a) CP @ TiO2 NPs		
10	98	16
25	86	34
50	63	62
75	42	80
100	24	98

(b) Aspirin (100)	20	96

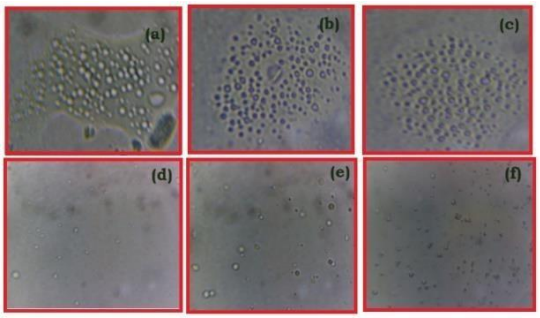

Fig. 11. Micrographs representing antiplatelet activity for different concentrations (µg/mL) of biosynthesized TiO2 NPs: (a) 10, (b) 25, (c) 50, (d) 75, (e) 100, and (f) control (Aspirin,

100 µg/mL).

Table - 13 details the antiplatelet activity of CP @ TiO_2 nanoparticles across various concentrations (10–100 µg/mL), comparing their efficacy with that of aspirin, a well-established antiplatelet medication. The data encompass the percentage of platelet aggregation alongside the corresponding percentage of aggregation inhibition.

In in vitro studies, at lower concentrations (10 µg/mL), CP @ TiO_2 nanoparticles demonstrated minimal inhibition (16%), allowing significant platelet aggregation (98%). However, as the concentration increased, platelet aggregation progressively decreased, indicating a more pronounced antiplatelet effect. At the highest concentration (100 µg/mL), CP @ TiO_2 nanoparticles exhibited maximum inhibition (98%), with only 24% platelet aggregation observed. These results suggest that TiO_2 nanoparticles could serve as a potent antiplatelet agent, although further investigation is necessary to assess their safety and efficacy in clinical applications.

In comparison, aspirin (100 µg/mL) inhibited platelet aggregation by 96%, demonstrating its established effectiveness in diminishing platelet aggregation. The increased inhibition percentage of CP @ TiO_2 nanoparticles with higher concentrations suggests a dose-dependent antiplatelet activity. These findings not only indicate the potential of CP @ TiO_2 nanoparticles as a robust antiplatelet agent but also inspire and motivate the audience with the potential therapeutic applications of these nanoparticles [37,38].

4. CONCLUSION

The current research illustrates the environmentally friendly method of synthesizing titanium dioxide (TiO_2) nanoparticles by utilizing *Costus pictus* D. leaf extract as a natural reducing and stabilizing agent. The optimized process results in consistent, spherical nanoparticles exhibiting a tetragonal crystalline formation. Characterization has identified bioactive compounds, including phenols and tannins, that contribute to the stability of the nanoparticles.

The TiO_2 nanoparticles exhibit exceptional characteristics that show potential for anticoagulant and antiplatelet functions. They outperform traditional agents like aspirin in specific tests, effectively inhibiting ADP-induced platelet aggregation. This observation indicates their potential in preventing thrombosis. Furthermore, they show dose-dependent anticoagulant properties by prolonging clotting times.

These findings underscore the potential biomedical applications of biosynthesized nanoparticles for cardiovascular health and the alignment of the green synthesis method with sustainability goals. However, to fully validate their role in biomedical science, future research should explore additional therapeutic uses, conduct in vivo studies, and perform long-term safety assessments.

5. ACKNOWLEDGEMENT

The authors wish to extend their heartfelt gratitude to the Centralized Instrumentation and Service Laboratory at Annamalai University for generously providing access to their lab facilities.

Disclosure Statement

Conflict of Interest: The authors declare no competing interests.

Ethical Approval*:* This study does not involve human participants or animals.

Informed Consent: None**.**

REFERENCES

[1] Chandra, Harish, Pragati Kumari, Elza Bontempi, and Saurabh Yadav. (2020). "Medicinal Plants: Treasure Trove for Green Synthesis of Metallic Nanoparticles and Their Biomedical Applications." Biocatalysis and Agricultural Biotechnology 24: 101518.

[2] Chandra, Harish, Deepak Patel, Pragati Kumari, J. S. Jangwan, and Saurabh Yadav. (2019). "Phyto-mediated Synthesis of Zinc Oxide Nanoparticles of Berberis Aristata: Characterization, Antioxidant Activity and Antibacterial Activity with Special Reference to Urinary Tract Pathogens." Materials Science and Engineering: C 102: 212-220.

[3] Irshad, Muhammad Atif, Rab Nawaz, Muhammad Zia Ur Rehman, Muhammad Adrees, Muhammad Rizwan, Shafaqat Ali, Sajjad Ahmad, and Sehar Tasleem. (2021). "Synthesis, Characterization and Advanced Sustainable Applications of Titanium Dioxide Nanoparticles: A Review." Ecotoxicology and Environmental Safety 212: 111978.

[4] Shi, Yongli, Feng Wang, Jibao He, Santosh Yadav, and He Wang. (2010). "Titanium Dioxide Nanoparticles Cause Apoptosis in BEAS-2B Cells through the Caspase 8/t-Bid- Independent Mitochondrial Pathway." Toxicology Letters 196 (1): 21-27.

[5] Selvakumarasamy, Saranya, Balakrishnaraja Rengaraju, Siddhu Adhiaman Arumugam, and Ramalakshmi Kulathooran. (2021). "Costus Pictus–Transition from a Medicinal Plant to Functional Food: A Review." Future Foods 4: 100068.

[6] Jayasri, M. A., S. Gunasekaran, A. Radha, and T. L. Mathew. (2008). "Anti-diabetic Effect of Costus Pictus Leaves in Normal and Streptozotocin-induced Diabetic Rats." International Journal of Diabetes and Metabolism 16 (3): 117-122.

[7] Hegde, Prakash K., Harini A. Rao, and Prasanna N. Rao. (2014). "A Review on Insulin Plant (Costus Igneus Nak)." Pharmacognosy Reviews 8 (15): 67.

[8] World Health Organization. (2013). WHO Traditional Medicine Strategy: 2014-2023. Geneva: World Health Organization.

[9] Kim, Jae Kyoun, Kyeong Han Kim, Yong Cheol Shin, Bo-Hyoung Jang, and Seong-Gyu Ko. (2020). "Utilization of Traditional Medicine in Primary Health Care in Low-and

[10] Middle-Income Countries: A Systematic Review." Health Policy and Planning 35 (8): 1070-1083.

[11] Meschia, James F., Cheryl Bushnell, Bernadette Boden-Albala, Lynne T. Braun, Dawn

[12] M. Bravata, Seemant Chaturvedi, Mark A. Creager (2014). "Guidelines for the Primary Prevention of Stroke: A Statement for Healthcare Professionals from the American Heart Association/American Stroke Association." Stroke 45 (12): 3754-3832.

[13] Shafaat, Omid, and Houman Sotoudeh. (2023). "Stroke Imaging." In StatPearls [Internet]. StatPearls Publishing.

[14] Şahin, Bayram, and Gülnur İlgün. (2022). "Risk Factors of Deaths Related to Cardiovascular Diseases in World Health Organization (WHO) Member Countries." Health & Social Care in the Community 30 (1): 73-80.

[15] Ngoepe, Nkgaetsi Marius, Morongwa Mary Mathipa, and Nomso Charmaine Hintsho- Mbita. (2020). "Biosynthesis of Titanium Dioxide Nanoparticles for the Photodegradation of Dyes and Removal of Bacteria." Optik 224: 165728.

[16] Birt, Diane F. (2006). "Phytochemicals and Cancer Prevention: From Epidemiology to Mechanism of Action." Cancer Prevention Research 20-21.

[17] Mishra, Vijaylaxmee, Richa Sharma, N. Dut Jasuja, and Deepak Kumar Gupta. (2014). "A Review on Green Synthesis of Nanoparticles and Evaluation of Antimicrobial Activity." International Journal of Green and Herbal Chemistry 3 (1): 081-094.

[18] Ramimoghadam, Donya, Samira Bagheri, and Sharifah Bee Abd Hamid. (2014). "Biotemplated Synthesis of Anatase Titanium Dioxide Nanoparticles via Lignocellulosic Waste Material." BioMed Research International 2014 (1): 205636.

[19] Bekele, Eneyew Tilahun, Bedasa Abdisa Gonfa, Osman Ahmed Zelekew, Hadgu Hailekiros Belay, and Fedlu Kedir Sabir. (2020). "Synthesis of Titanium Oxide Nanoparticles Using Root Extract of Kniphofia Foliosa as a Template, Characterization, and Its Application on Drug Resistance Bacteria." Journal of Nanomaterials 2020 (1): 2817037.

[20] Narayanan, Mathiyazhagan, Paramasivam Vigneshwari, Devarajan Natarajan, Sabariswaran Kandasamy, Mishal Alsehli, Ashraf Elfasakhany, and Arivalagan Pugazhendhi. (2021). "Synthesis and Characterization of

TiO2 NPs by Aqueous Leaf

[21] Extract of Coleus Aromaticus and Assess Their Antibacterial, Larvicidal, and Anticancer Potential." Environmental Research 200: 111335.

[22] Ahmad, Waseem, Krishna Kumar Jaiswal, and Shivani Soni. (2020). "Green Synthesis of Titanium Dioxide (TiO2) Nanoparticles by Using Mentha Arvensis Leaves Extract and Its Antimicrobial Properties." Inorganic and Nano-Metal Chemistry 50 (10): 1032-1038.

[23] Rajkumari, J., C. Maria Magdalane, B. Siddhardha, J. Madhavan, G. Ramalingam, Naif Abdullah Al-Dhabi, Mariadhas Valan Arasu, A. K. M. Ghilan, V. Duraipandiayan, and

[24] K. Kaviyarasu. (2019). "Synthesis of Titanium Oxide Nanoparticles Using Aloe Barbadensis Mill and Evaluation of Its Antibiofilm Potential Against Pseudomonas Aeruginosa PAO1." Journal of Photochemistry and Photobiology B: Biology 201: 111667.

[25] Subhapriya, S., and P. J. M. P. Gomathipriya. (2018). "Green Synthesis of Titanium Dioxide (TiO2) Nanoparticles by Trigonella Foenum-Graecum Extract and Its Antimicrobial Properties." Microbial Pathogenesis 116: 215-220.

[26] Rajeshkumar, S., J. Santhoshkumar, Leta Tesfaye Jule, and Krishnaraj Ramaswamy. (2021). "Phytosynthesis of Titanium Dioxide Nanoparticles Using King of Bitter Andrographis Paniculata and Its Embryonic Toxicology Evaluation and Biomedical Potential." Bioinorganic Chemistry and Applications 2021 (1): 6267634.

[27] Ansari, Afzal, Vasi Uddin Siddiqui, Wahid Ul Rehman, Md Khursheed Akram, Weqar Ahmad Siddiqi, Abeer M. Alosaimi, Mahmoud A. Hussein, and Mohd Rafatullah. (2022). "Green Synthesis of TiO2 Nanoparticles Using Acorus Calamus Leaf Extract and Evaluating Its Photocatalytic and In Vitro Antimicrobial Activity." Catalysts 12 (2): 181.

[28] Nabi, G., Majid, A., Riaz, A., Alharbi, T., Kamran, M.A., and Al-Habardi, M. (2021). "Green Synthesis of Spherical TiO2 Nanoparticles Using Citrus Limetta Extract: Excellent Photocatalytic Water Decontamination Agent for RhB Dye." Inorganic Chemistry Communications 129: 108618.

[29] George, John, C. C. Gopalakrishnan, P. K. Manikuttan, K. Mukesh, and S. Sreenish. (2021). "Preparation of Multi-purpose TiO2 Pigment with Improved Properties for Coating Applications." Powder Technology 377: 269-273.

[30] Al Masoudi, Luluah M., Abeer S. Alqurashi, Abeer Abu Zaid, and Hamida Hamdi. (2023). "Characterization and Biological Studies of Synthesized Titanium Dioxide

[31] Nanoparticles from Leaf Extract of Juniperus Phoenicea L. Growing in Taif Region, Saudi Arabia." Processes 11 (1): 272.

[32] Shimi, Annin K., Hiwa M. Ahmed, Muhammad Wahab, Snehlata Katheria, Saikh Mohammad Wabaidur, Gaber E. Eldesoky, Md Ataul Islam, and Kantilal Pitamber Rane. (2022). "Synthesis and Applications of Green Synthesized TiO2 Nanoparticles for Photocatalytic Dye Degradation and Antibacterial Activity." Journal of Nanomaterials 2022 (1): 7060388.

[33] Ilango, Saraswathi, Saikumar Pindigiri, Sembulingam Kandhaswamy, and Saikarthik Jayakumar. (2020). "Preliminary Phytochemistry, Gas Chromatography–Mass Spectrometry, and High-Performance Thin-Layer Chromatography Fingerprint Analysis of Ethanol Extract of Costus Speciosus Rhizomes and Its Therapeutic Implications." Drug Invention Today 13 (7): 1204-1211.

[34] Kanthal, Lakshmi Kanta, Akalanka Dey, K. Satyavathi, and P. J. P. R. Bhojaraju. (2014). "GC-MS Analysis of Bio-active Compounds in Methanolic Extract of Lactuca Runcinata DC." Pharmacognosy Research 6 (1): 58.

[35] Ruslan and Ariyansyah. (2019). "Biosynthesis of Titanium Dioxide Using Sargassum sp.

[36] Seaweed Extract Under Microwave." International Journal of Applied Chemistry (2).

[37] Ayouni, Karima, Meriem Berboucha-Rahmani, Hye Kyong Kim, Djebbar Atmani, Rob Verpoorte, and Young Hae Choi. (2016). "Metabolomic Tool to Identify Antioxidant Compounds of Leaf and Fraxinus Angustifolia Stem Bark Extracts." Industrial Crops and Products 88: 65-77.

[38] Vinotha, Viswanathan, Arokiadhas Iswarya, Rajagopalan Thaya, Marimuthu Govindarajan, Naiyf S. Alharbi, Shine Kadaikunnan, Jamal M. Khaled, Mohammed N. Al-Anbr, and Baskaralingam Vaseeharan. (2019). "Synthesis of ZnO Nanoparticles Using Insulin-Rich Leaf Extract: Anti-Diabetic, Antibiofilm and Antioxidant Properties." Journal of Photochemistry and Photobiology B: Biology 197: 111541.

[39] Elegbede, J. A., A. Lateef, M. A. Azeez, T. B. Asafa, T. A. Yekeen, I. C. Oladipo, D. A. Aina, L. S. Beukes, and E. B. Gueguim-Kana. (2020). "Biofabrication of Gold Nanoparticles Using Xylanases Through

Valorization of Corncob by Aspergillus Niger and Trichoderma longibrachiatum: Antimicrobial, Antioxidant, Anticoagulant and Thrombolytic Activities." Waste and Biomass Valorization 11: 781-791.

[40] Prandoni, Paolo, Anna Falanga, and Andrea Piccioli. (2007). "Cancer, Thrombosis and Heparin-Induced Thrombocytopenia." Thrombosis Research 120: S137-S140.

[41] Kim, Hee Kyeong, Myung-Jin Choi, Song-Hyun Cha, Yean Kyoung Koo, Sang Hui Jun, Seonho Cho, and Youmie Park. (2013). "Earthworm Extracts Utilized in the Green Synthesis of Gold Nanoparticles Capable of Reinforcing the Anticoagulant Activities of Heparin." Nanoscale Research Letters 8: 1-7.

[42] Lingaraju, K., R. B. Basavaraj, K. Jayanna, S. Bhavana, S. Devaraja, HM Kumar Swamy,

[43] G. Nagaraju, H. Nagabhushana, and H. Raja Naika. (2021). "Biocompatible Fabrication of TiO2 Nanoparticles: Antimicrobial, Anticoagulant, Antiplatelet, Direct Hemolytic and Cytotoxicity Properties." Inorganic Chemistry Communications 127: 108505.

[44] Krishnaraj, R. Navanietha, and Sheela Berchmans. (2013). "In Vitro Antiplatelet Activity of Silver Nanoparticles Synthesized Using the Microorganism Gluconobacter Roseus: An AFM-Based Study." RSC Advances 3 (23): 8953-8959.

[45] Dakshayani, S. S., M. B. Marulasiddeshwara, Sharath Kumar, Ramesh Golla, S. R. H. K. Devaraja, and Rashmi Hosamani. (2019). "Antimicrobial, Anticoagulant and Antiplatelet Activities of Green Synthesized Silver Nanoparticles Using Selaginella (Sanjeevini) Plant Extract." International Journal of Biological Macromolecules 131: 787-797.

-.